

Theoretical and experimental results for *p*-type GaAs electrolyte electroreflectance

R. A. Batchelor, A. C. Brown, and A. Hamnett

Inorganic Chemistry Laboratory, South Parks Road, Oxford OX1 3QR, England

(Received 5 July 1989)

The intermediate-field (effective-mass) theory is used to predict the electroreflectance of *p*-type GaAs as a function of space-charge voltage and dopant density. The effect of the inhomogeneous electric field in the space-charge layer is included by modeling as reflection from a series of thin films, and the transition oscillator strength is determined by comparison with the published optical properties of GaAs. The extent of thermal broadening is determined by comparison with experimental electrolyte electroreflectance (EER) spectra which were measured for 2×10^{16} , 7×10^{16} , 4×10^{17} , and $2 \times 10^{18} \text{ cm}^{-3}$ doped *p*-type GaAs in $0.5M \text{ H}_2\text{SO}_4(\text{aq})$ and $1.0M \text{ KOH}(\text{aq})$ by holding the electrodes at a dc potential and adding an ac modulation of 15 mV. Agreement with theory is sufficiently good for us to be able to measure the space-charge voltage in electrodes by comparison of experimental EER line shapes with theory and thereby to deduce the presence of partial Fermi-level pinning in the $7 \times 10^{16} \text{ cm}^{-3}$ samples which we measured, an interpretation that was supported by the unusually unstable impedance behavior of electrodes made from this crystal.

INTRODUCTION

The original work of Brattain and Garrett in 1955 (Ref. 1) on the semiconductor-electrolyte interface introduced the model of the potential distribution at such interfaces which is still in use today. This model was based on the theory of the semiconductor-metal junction developed by Mott² and Schottky³ when a semiconductor electrode is reverse biased, a space-charge layer, depleted of charge carriers, extends into the semiconductor. As the charge-carrier density in the electrode is lower than that in any reasonably concentrated electrolyte, the change in applied potential should be dropped entirely within this space-charge layer.⁴ However, even Brattain and Garrett questioned the assumption that the space-charge layer was the sole region of the interface sensitive to changes in the applied potential and pointed out that charge localized at the surface in "surface states" could reduce the electric field in the space-charge layer. Where the concentration of surface charge or the coverage of surface dipoles changes with applied potential, then only a fraction of that change of potential will be dropped across the space-charge layer.

More than 30 years later the electrochemistry of a huge range of single-crystal and polycrystalline semiconductors has been studied, a scientific program whose primary impulse was the discovery in 1971 by Fujishima and Honda⁵ of the photoelectrolysis of water on rutile. A whole battery of techniques has now been brought to bear on the semiconductor-electrolyte interface: photovoltage, photocurrent, and impedance studies, in particular, being used in an attempt to elucidate its potential distribution. The results from these studies often show behavior that deviates markedly from the classical models, and it has become clear that it is extremely difficult unambiguously to determine the potential distribution from measurements of current or voltage responses. Impedance measurements are very sensitive to any rapid faradaic pro-

cesses at the surface, although these may not affect the dc potential distribution significantly. For photocurrent studies, electron-hole recombination is a major theoretical problem in the analysis of data, especially close to the flat-band potential.⁶ A technique is needed which can measure the voltage drop within the depletion layer more directly.

This work intends to show that electrolyte electroreflectance (EER) can be used to measure the voltage drop across the depletion layer, V_{SC} . A small ac potential modulation is applied to the semiconductor and the resulting modulation of the reflectance spectrum is measured. By using a sufficiently small modulation in EER, we show that it is possible to determine the dc potential drop across the depletion layer. The basic theory of semiconductor electroreflectance has been known for some time,⁷ but the complexity of the resulting equations has hindered the use of this technique to measure the voltage drop across the space-charge region, V_{SC} . In the case of small electric fields and high thermal broadening, the normalized spectra $\Delta R/R$ will have a simple third-derivative form that does not vary with space-charge voltage. Due to its ease of application, the third-derivative approach has predominated in the use of EER to characterize semiconductor surfaces in electrolyte. However, for the dopant densities of greatest interest in electrochemical studies, 10^{16} – 10^{18} cm^{-3} , it is clear that this model is often not applicable, since the line shape changes with applied potential. By applying the more general intermediate-field theory, we should be able to model the EER spectrum for a given sample and then predict the spectral variation with voltage. Success in this program was also found to depend on inclusion of the effect due to the *variation* of the electric field in the depletion layer. The Mott-Schottky model predicts that this field will vary linearly from the surface of the semiconductor to the edge of the depletion layer. As a result, the dielectric function varies on moving from the surface

and this is modeled by a multilayer reflection algorithm.

In this work the EER has been measured for four $\langle 100 \rangle$ p -type GaAs samples of dopant density from 2×10^{16} to $2 \times 10^{18} \text{ cm}^{-3}$ in $0.5M \text{ H}_2\text{SO}_4$ and $1.0M \text{ KOH}$. The impedance of these samples was also studied over a range of frequencies. p -type gallium arsenide was especially suitable for this work because its extensively studied electrochemistry⁸ allowed us to check that the p -type GaAs electrode was behaving as expected in each of our experimental conditions. Moreover, its well-characterized optical and electronic properties allow spectra to be modeled theoretically, with only the effect of thermal broadening to be determined by comparison with experiment.

THEORETICAL APPROACH

Electroreflectance spectra result from the effect of an electric field on the optical properties of the semiconductor in the surface region. The theory for the effect of an electric field on the optical properties of a semiconductor has been known for some time,^{9,10} and we follow the theory already described in its application to semiconductor electrochemistry.¹¹ Electroreflectance has been widely used in the characterization of semiconductor band structure and is now applied in the study of multilayer quantum wells using a quite different theoretical approach.¹² It is also the basis of the photoreflectance effect where semiconductor reflectance is modulated by illumination of the surface with a chopped laser beam. The variation in light intensity at the surface modulates the charge distribution, and therefore, the electric field near the surface.¹³

By assuming that the electric field is too small for interband tunneling to occur and neglecting the electron-hole interaction, the imaginary part of the dielectric function at the absorption onset will be given by

$$\epsilon_2(\omega) = \frac{B\theta^{1/2}\pi}{\omega^2} [\text{Ai}'^2(x) - x \text{Ai}^2(x)], \quad (1)$$

where

$$x = (\omega_g - \omega)/\theta, \quad \theta = (\mathcal{E}^2 e^2 / 2\mu\hbar)^{1/3}$$

within the effective-mass approximation. \mathcal{E} is the electric field, μ is the joint effective mass in the direction of the applied field, and $\text{Ai}(z)$ is the Airy function regular at infinity.¹⁴ B contains the effect of matrix elements on the transition. The zero-field limit of Eq. (1) is

$$\epsilon_2(\omega) = \frac{B}{\omega^2} (\omega - \omega_g)^{1/2} u(-x), \quad (2)$$

where $u(x)$ is the unit-step function. Equation (2) is the well-known result for a direct allowed transition in the absence of an electric field. Subtraction of (2) from (1) gives the change in $\epsilon_2(\omega)$ due to the electric field, $\Delta\epsilon_2(\omega)$. The quantity $\Delta\epsilon_2(\omega)$ is only substantial close to the critical point so that integration of the Kramers-Kronig equation⁹ should yield an accurate value for the change in the real part of the dielectric function $\Delta\epsilon_1(\omega)$:

$$\Delta\epsilon_1(\omega) = \frac{B\theta^{1/2}\pi}{\omega^2} [\text{Ai}'(x)\text{Bi}'(x) - x \text{Ai}(x)\text{Bi}(x)] + \frac{Bx^{1/2}}{\omega^2} u(x). \quad (3)$$

The effect of lifetime-induced uncertainty in the energy of the excited state can be included by Lorentzian broadening of $\Delta\epsilon_2$ and $\Delta\epsilon_1$. This has been done by combining the electro-optic functions:

$$F = \pi [\text{Ai}'^2(x) - x \text{Ai}^2(x)] - (-x)^{1/2} u(-x),$$

$$G = \pi [\text{Ai}'(x)\text{Bi}'(x) - x \text{Ai}(x)\text{Bi}(x)] + x^{1/2} u(x),$$

to give

$$F + iG = \pi [\text{Ai}'^2(x) - x \text{Ai}^2(x)]$$

$$+ i\pi [\text{Ai}'(x)\text{Bi}'(x) - x \text{Ai}(x)\text{Bi}(x)] + ix^{1/2}.$$

The Lorentzian broadening of $F + iG$ can then be calculated by integration about the infinite semicircle in the upper half of the complex plane.⁹ The Lorentzian integral disappears on the arc of the semicircle in the upper half of the complex plane and can therefore be equated to $2\pi i$ multiplied by the residue of the pole at $\chi = x + i\Gamma/\theta$. Writing $F + iG$ as $H(x)$, we have

$$H(x, \Gamma) = \left[\frac{\Gamma/\theta}{\pi} \right] \int_{-\infty}^{\infty} \frac{H(\chi)}{(\chi - x)^2 + \Gamma^2/\theta^2} d\chi = H(x + i\Gamma/\theta).$$

Defining $z = (\omega_g - \omega + i\Gamma)/\theta$, the broadened electro-optic functions $F(z)$ and $G(z)$ can then be obtained by equating to the real and imaginary parts of $H(z)$. We have extended this treatment by including the factor of $1/\omega^2$ from the expressions for $\Delta\epsilon_2$ and $\Delta\epsilon_1$ in the broadening process, so that we use

$$\Delta\epsilon_2(z) = B\theta^{1/2} \text{Re} \left[\frac{H(z)}{(\omega - i\Gamma)^2} \right],$$

$$\Delta\epsilon_1(z) = B\theta^{1/2} \text{Im} \left[\frac{H(z)}{(\omega - i\Gamma)^2} \right].$$

The numerical difficulty in calculating Airy functions of complex argument had led to the use of asymptotic forms of the equations in many published results. Aspnes showed that where the effect of lifetime broadening on the electron energy was much greater than that of the electric field $3\hbar\Omega \ll \Gamma$, where $\Omega = 2^{-2/3}\theta$, the expression for $\Delta\tilde{\epsilon}(\omega, \mathcal{E})$ reduces to a simple third-derivative form.¹⁵ The predicted line shape is independent of the applied potential, and its amplitude is proportional to the modulation of the square of the electric field, and is therefore linear in the modulation of the applied potential. Owing to its ease of application, Aspnes's third-derivative expression for $\Delta\tilde{\epsilon}(\omega)$ has been the dominant interpretative approach for electroreflectance, although it is less valuable for more highly doped semiconductors, where the depletion-layer fields are large, and also less useful at the absorption threshold, where Γ is smaller. Aspnes termed this the low-field limit, and the more-general approach

presented above is termed the intermediate-field theory. The high-field case applies where the field modifies the band structure significantly and interband tunneling starts to occur. Bennett and Soref have recently used the intermediate-field approach to estimate the effect of electric fields below the band gap on the optical properties of some III-V compound semiconductors, including gallium arsenide.¹⁶ In this work we apply the intermediate-field theory to interpret the changes in gallium arsenide EER with applied potential and with dopant density. The Airy and related functions of complex argument are readily evaluated by our high-precision FORTRAN routines.

The theory presented so far has not considered some important features of the semiconductor-electrode-electrolyte interface. The most important is that the electric field within the depletion layer is not constant, but decreases linearly with distance from the surface. The changing electric field within the depletion layer is particularly important for band-gap transitions as the absorption coefficient of the light is sufficiently low for light to penetrate right through the depletion layer for some wavelengths. Aspnes has treated this problem by a perturbation approach in the case of normal incidence.¹⁷ This approach has been used to interpret the electroreflectance of *p*-type InP by assuming that the limiting case of $KW \ll 1$ is applicable, where K is the light propagation vector, W is the width of the space-charge region, and the effect of absorption is neglected.¹⁸ However, the assumption $KW \ll 1$ is not applicable to our study of $2 \times 10^{16} \text{ cm}^{-3}$ *p*-type GaAs as we estimate $K \sim 2.68 \times 10^7 \text{ m}^{-1}$ at 850 nm for GaAs; if the semiconductor is 1.0 V from flat-band potential, then the depletion-layer width will be $W \sim 1.91 \times 10^{-7} \text{ m}$ and $KW \sim 5.12$. A more accurate model for the effect of the potential distribution on the electroreflectance is needed to interpret such data fully.

Instead we have modeled reflection from the depletion layer as from a series of thin films. The field is taken as uniform in each film and is determined by its distance from the electrode surface. The effect of the electric field on the dielectric function of each film is assumed to be the same as the effect of that field on bulk GaAs. The change in dielectric function can then be calculated for each film so that the total reflection of incident light at any angle or polarization can then be calculated by a multilayer-reflection routine. If a large enough number of very thin films is used, the result will converge to the solution for the effect of an inhomogeneous dielectric function on the reflectance.¹⁹ In practice, between 12 and 20 layers have been found to be sufficient. An important feature of taking the space-charge-layer electric-field inhomogeneity into account is that some EER spectra are predicted to be very different in shape to the electro-optic functions evaluated by Aspnes.

The use of the equations for the Franz-Keldysh effect within the layers neglects any distortion of the wave function due to the changing of the electric field in the depletion layer. Such a distortion would prevent the optical response of a point in the depletion layer from being characterized by a local dielectric function, as the response would also be affected by the electric fields in

the rest of the semiconductor which would contribute to the determination of the wave function. Del Sole and Aspnes have considered the effect of a varying electric field on the wave function within the WKB approximation and the nonlocal dielectric function which would result from this.^{20,21} A self-consistent solution to this problem would require a considerable increase in numerical complexity and is beyond the scope of this paper. We would not expect the assumption of bulk electro-optic behavior within the layers to be a major problem, as the electric field changes relatively slowly with distance on an atomic scale. However, the approximation will become less accurate for more highly doped semiconductors, where the depletion layer is smaller and the electric field changes more rapidly with distance.

Our quantitative approach to reflection reveals that $\Delta R/R$ is not sensitive to thin nonabsorbing layers on the surface or to perturbations in the potential distribution close to the surface. If very large electric fields are present in the top few monolayers of GaAs, then the model predicts that they will have little effect on $\Delta R/R$ provided that the potential distribution in the rest of the depletion layer is unaltered. If a significant proportion of the depletion-layer voltage is dropped within this surface layer, then EER similar to that for a classical depletion layer with a smaller voltage drop across it is predicted. The insensitivity of $\Delta R/R$ to large electric fields within a few monolayers of the surface is not surprising as we expect reflection intensity to be most sensitive to changes which occur over distances of the order of a wavelength.

The effect of lifetime broadening has been modeled by inclusion of Γ , but this quantity is likely to vary with the excitation energy. Higher-energy electrons in the conduction band will undergo more rapid relaxation due to phonon emission and collision with lattice defects, so that $\Gamma(\omega)$ is likely to increase with ω . We propose an empirical variation of $\Gamma = \Gamma_0 \exp \delta(\omega - \omega_g)$, where δ must be determined by fitting to experimental spectra. In practice, our proposed function for $\Gamma(\omega)$ is quite effective as δ can be determined from one spectrum and then fixed, so that the voltage variation can be predicted without the use of any undetermined parameters.

If we incorporate all of the above features into our model, then a surprising result is found: even in situations where the low-field model is clearly inapplicable, it is still found that, provided the ac modulation is small, $\Delta R/R$ should increase linearly with the modulation amplitude. The linear relationship between $\Delta R/R$ and modulation amplitude was observed in our experimental work over ranges of modulation voltage considerably larger than that used for spectra presented here [15 mV rms]. Thus, the linearity of $\Delta R/R$ with modulation voltage cannot be used to demonstrate low-field conditions. However, it allows us to calculate the rms of the sinusoidal variation of $\Delta R/R$ from the difference of two dc values:

$$\frac{\Delta R(\text{ac rms})}{R} = \frac{\Delta R(V_{\text{dc}+\text{ac}}) - \Delta R(V_{\text{dc}})}{R},$$

where V_{dc} is the dc voltage across the depletion layer and V_{ac} is the rms of the ac modulation.

Our treatment neglects the effect of electron-hole in-

teractions which have been invoked to interpret the electroreflectance of many materials. Silberstein and Polak interpreted the EER of the $\langle 111 \rangle$ face n -type GaAs at 300 K at the band gap as due to exciton quenching which caused the shape of the feature to change with applied potential.^{22,23} Apart from the sharp shape of the feature, the evidence cited for this assignment was that the signal size at 880 nm oscillates with applied potential. The oscillation is believed to result from the modulation of the size of the region close to the surface where excitons are dissociated by the electric field. Light reflected from the surface will undergo interference with light reflected from the dissociation-region–bulk boundary, and this will be sensitive to the size of the dissociation region which is controlled by the applied potential. However, our model predicts a similar oscillation of $\Delta R/R$ with depletion-layer voltage due to interference effects in the inhomogeneous field, although the magnitude of $\Delta R/R$ should decrease with increasing depletion. In fact, the EER which we have obtained on $\langle 100 \rangle$ p -type GaAs at 300 K seems to be interpretable without invoking exciton effects.

Another effect that we have not treated here is that of defects within the depletion layer, which are likely to result in a distortion of the electric field about the defect. Theoretical treatments of the effect of defect-induced field distortion have been presented,²⁴ and Raccach has incorporated the effect into a generalized low-field theory which he has applied to the EER of CuInSe₂ samples.²⁵ However, there would be considerable difficulties extending this treatment in any simple way to the intermediate-field regime, and we have taken the view that *only after all possible intermediate-field effects have been eliminated as explanation of the observed EER spectra should we consider this type of effect.* As we shall see, for $\langle 100 \rangle$ p -type GaAs the essential features of the EER spectra are interpretable within the intermediate-field model.

Experimental and theoretical work on the EER of an n -type GaAs sample has already been interpreted by our approach.²⁶ However, in this paper we have used a much more accurate description of the zero-field optical properties of the semiconductor, and as a result, our theoretical line shapes are essentially quantitative.

DETERMINATION OF PARAMETERS USED IN THE MODEL

The dopant densities of the $\langle 100 \rangle$ p -type GaAs samples as measured by the Hall effect were compared with those obtained from Mott-Schottky plots to give the values used. The two methods were in surprisingly close agreement for three of the samples, but for the electrode where Hall-effect measurements gave $N_A = 4.4 \times 10^{17} \text{ cm}^{-3}$, the impedance data gave $N_A = 2.7 \times 10^{17} \text{ cm}^{-3}$. The latter value was used initially, since deviations from Mott-Schottky behavior are more likely to result in overestimation of dopant density.

The joint effective mass μ_i is obtained from the electron effective mass in the conduction band, m_{ci} and the hole effective mass in the valence band, m_{vi} :

$$\frac{1}{\mu_i} = \frac{1}{m_{ci}} - \frac{1}{m_{vi}}.$$

However, there are two bands of different hole effective mass at the valence-band edge, so the joint effective mass is calculated for both the light- and heavy-hole bands to give $\mu_{hh} = 0.058m_e$ and $\mu_{lh} = 0.034m_e$ from literature values.²⁷ A full treatment of the effect of degeneracy at the Γ point on the electroreflectance of III-V compound semiconductors would be complex, and the two approaches usually adopted are either to use a single average effective mass or to consider the effect of the two bands independently. Seraphin and Bottka²⁸ considered only the heavy-hole contribution to electroreflectance of GaAs. Chandreskhar and Pollak²⁹ supported the validity of this approach by measurement of the effect of uniaxial stress on the electroreflectance (ER) spectrum of GaAs. Bardeen³⁰ used a sum-rule calculation to estimate the relative strengths of absorption from the light- and heavy-hole valence bands. Bennett and Soref¹⁶ applied this approach to calculate electroabsorption and refraction for GaAs for wavelengths beneath the band gap. We use the recent full-zone $\mathbf{k} \cdot \mathbf{p}$ calculation of Wysin *et al.*³¹ to estimate the ratio of absorption strengths by the two valence bands as $B_{lh} : B_{hh} = 1:2$ and then consider the contribution of the two bands as independent. Spectra were also modeled using single effective masses between $0.047m_e$ and $0.058m_e$. In fact, the differences between the two approaches are fairly small, although a significant qualitative effect is that independent inclusion of the contributions of light and heavy valence bands leads to interference and cancellation between the higher-energy oscillations of $\Delta R/R$ for $2 \times 10^{16} \text{ cm}^{-3}$ doped GaAs, giving theoretical spectra closer to the shape of those measured. The $E_0 + \Delta$ absorption at 1.765 eV results from a single valence-band split from the two others by spin-orbit coupling so only one hole effective mass needs to be considered. We therefore calculate a joint effective mass of $0.0446m_e$. The literature band gap of 1.425 eV is used in the model.²⁷

In attempting to model accurately the effect of the inhomogeneous field on reflection, it is important that accurate values are available for the optical properties of gallium arsenide at each wavelength. Fortunately, extensive measurements have been made on gallium arsenide,^{32–35} and we interpolate numerically between the published values to obtain the appropriate complex refractive index at each wavelength. Ellipsometric measurements on the samples in both acid and alkaline electrolyte confirmed that the electrodes were free from surface layers and that $n + ik$ coincided with the published values. The expression for $\epsilon_2(\omega)$, Eq. (2), is fitted to the reported values in the range of the absorption onset in order to determine the constant $B = B_{lh} + B_{hh}$ as $6.0 \text{ (eV)}^{3/2}$.

EXPERIMENTAL

The apparatus used is shown schematically in Fig. 1. Light from a 100-W tungsten lamp is passed through a programmable monochromator, of spectral half-width 5

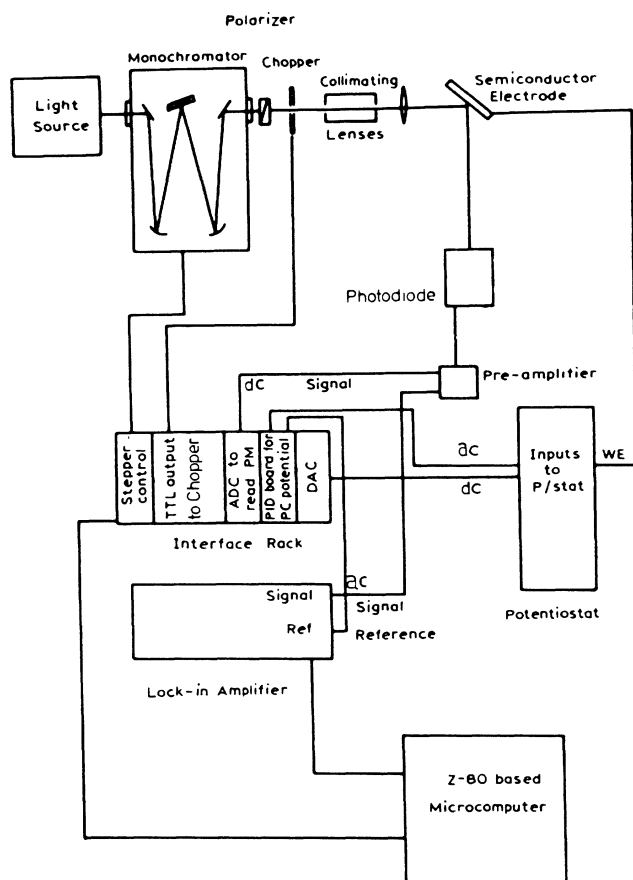


FIG. 1. Schematic diagram of computer-driven electroreflectance experiment.

nm, and then focused on the semiconductor electrode at 45° incidence. The electrode is positioned in an electrochemical cell with quartz windows that are perpendicular to the incident and reflected beams. The monochromatic light is predominantly *s* polarized. This gave spectra identical in shape to *p*-polarized light, although they were of half the magnitude, as predicted by differentiation of the Fresnel equations or by the more complicated multilayer-reflection routine which we use here. A dc potential is applied to the semiconductor to which a 15-mV (rms), 440-Hz sinusoidal modulation is added. Spectra could be measured over modulation frequencies 40 to 1000 Hz and no frequency dependence was observed within this range.

The reflected light is detected by a high-speed Si photodiode, the signal is amplified and then the ac component ΔR is measured by phase-sensitive detection. ΔR is then divided by the measured dc component from which a background value has been subtracted, to give the rms of the reflected intensity modulation $\Delta R/R$. The amplification and measurement of $\Delta R/R$ was checked to be quantitative by testing with a model input current of a similar size to that obtained from the photodiode during a typical EER experiment.

$\langle 100 \rangle$ slices of Zn-doped *p*-type GaAs were obtained from MCP Electronic Materials, who quoted Hall-effect

dopant densities of 2.3×10^{16} , 7.0×10^{16} , 4.4×10^{17} , and $2.0 \times 10^{18} \text{ cm}^{-3}$. The GaAs was polished on 3- μm , then 1- μm -Hyprez diamond paste and then washed in tetrahydrofuran (THF) followed by methanol. The samples were etched for three 10-s periods in 2% bromine-methanol. Low-resistance Ohmic contacts of indium zinc alloy were attached to the back of the electrode by heating for 5 min at 450°C under flowing 20 vol % H_2 and 80 vol % Ar. Wire was then glued to the back of the electrode by conducting silver araldite. The electrode was mounted at the end of a glass tube and sealed with araldite glue. Dark and illuminated cyclic voltammograms were taken of all electrodes, as well as impedance measurements for the frequency range 40–10000 Hz over the full range of stable potentials, typically -0.4 to -1.6 V versus $\text{Hg}/\text{Hg}_2\text{SO}_4$ in acid and -0.8 to -1.8 V versus Hg/HgO in alkali. Impedance results were interpreted in terms of both two- and five-component models.⁶

All solutions were prepared from pyrolyzed water according to the method of Conway³⁶ using Aristar-grade reagents and were continuously purged with argon throughout all measurements. In $0.5M \text{ H}_2\text{SO}_4(\text{aq})$ a reference electrode of $\text{Hg}/\text{Hg}_2\text{SO}_4$ in $1.0M \text{ H}_2\text{SO}_4(\text{aq})$ was used which had an electrode potential of $+0.41$ V compared to a commercial standard calomel electrode (SCE). In $1M \text{ KOH}(\text{aq})$ the reference electrode of Hg/HgO in $1.0M \text{ KOH}(\text{aq})$ was measured as -0.98 V versus SCE. Both reference potentials were checked periodically over the course of the experiments.

RESULTS

Reproducible, complete sets of EER spectra were obtained over the full range of potentials in which Faradaic currents were small, for all four dopant densities in both acid and alkaline solutions. By taking readings on freshly etched electrodes and sweeping the potential away from flat band, it was possible to obtain linear Mott-Schottky plots with little frequency dispersion in the range 10000–800 Hz for the samples in acid. The dopant densities obtained from the plots agreed closely with the manufacturer's values which are measured by the Hall Effect.

It is clear that even the spectra for the lowest-doped sample (Fig. 2) are not in the low-field limit, even close to the flat-band potential of $+0.0$ V versus $\text{Hg}_2\text{SO}_4/\text{Hg}$ in $1M \text{ H}_2\text{SO}_4(\text{aq})$. The first Franz-Keldysh oscillation is clearly seen, some structure on the low-energy positive peak is just resolvable, and the line shape changes with applied potential. The linear relationship between the signal size and small (< 50 mV) modulation amplitudes was observed as predicted by our model.

EER for GaAs in $0.5M \text{ H}_2\text{SO}_4(\text{aq})$

The spectra taken in acid solution are interpreted first, as these results were found to be more reproducible and to undergo a smoother change with applied potential. The model was fitted to the spectrum for $2 \times 10^{16} \text{ cm}^{-3}$ at -1.0 V from the impedance-measured flat-band potential of 0.0 V vs $\text{Hg}/\text{Hg}_2\text{SO}_4$. Initially we took Γ as 0.050 eV as this had been determined by earlier EER work on *n*-

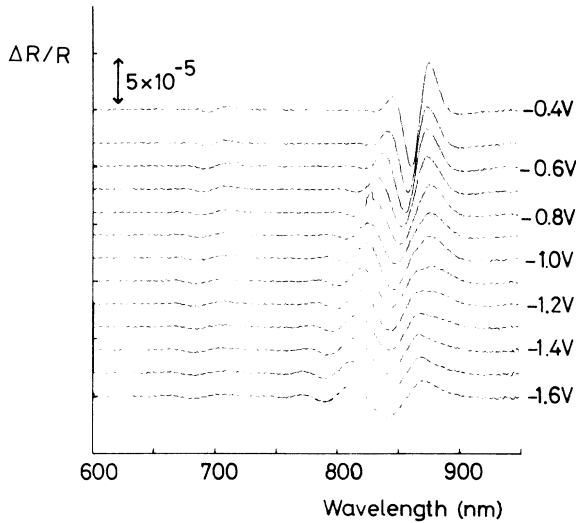


FIG. 2. Experimental EER spectra for $2 \times 10^{16} \text{ cm}^{-3}$ *p*-type GaAs in $0.5M \text{ H}_2\text{SO}_4(\text{aq})$ obtained with 15-mV, 440-Hz modulation. The potentials given are with respect to the Hg/Hg₂SO₄ reference electrode.

type GaAs in aqueous solution.²⁶ This gave a theoretical spectrum which was a factor of 2 smaller than experiment and had rather formless peaks with the wrong size ratio. Γ was therefore reduced to 0.010 eV at the transition onset in order to reproduce the sharp EER peaks near the optical threshold and was then allowed to increase fairly rapidly with energy, according to $\Gamma = \Gamma_0 \exp[\delta(\omega - \omega_g)]$. This gave main peaks of the correct size and shape ratio, and by setting $\delta = 5 \text{ eV}^{-1}$ the Franz-Keldysh oscillations are emulated with considerable success. The value of Γ_0 is smaller than that usually used in interpretation of room-temperature electroreflectance, but larger than that normally used in the interpretation of exciton broadening processes³⁷ or sometimes measured in photoreflectance.¹³

Most EER spectra are interpreted in terms of the low-field model, and if this does not strictly apply or if Γ increases with ω , then Γ_0 will be overestimated. The mean

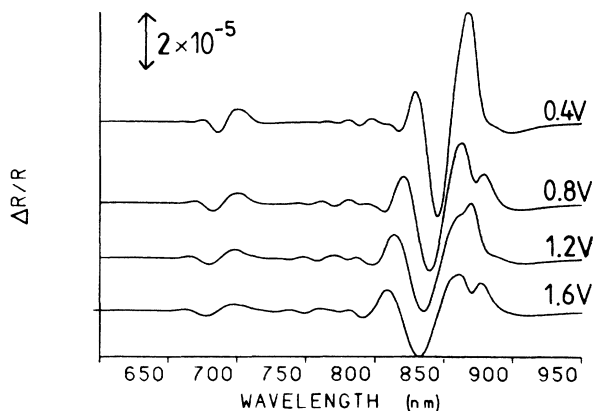


FIG. 3. Theoretical EER spectra for $2 \times 10^{16} \text{ cm}^{-3}$ *p*-type GaAs for various space-charge voltages. Calculated using $\Gamma_0 = 0.010$, $\delta = 5 \text{ eV}^{-1}$, and a modulation voltage of 15 mV.

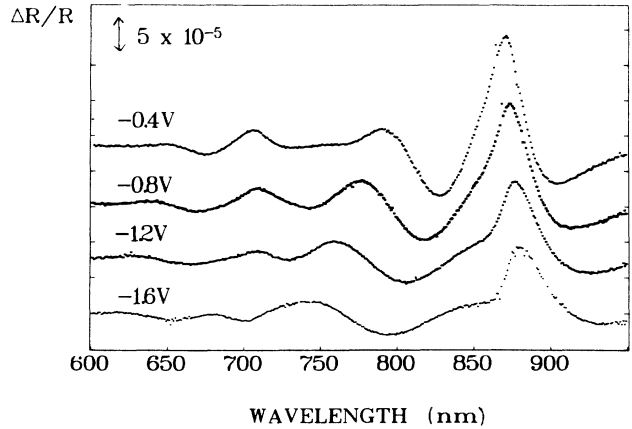


FIG. 4. Experimental EER spectra for a $4.4 \times 10^{17} \text{ cm}^{-3}$ (Hall effect)/ $2.7 \times 10^{17} \text{ cm}^{-3}$ (Mott-Schottky plot) *p*-type GaAs electrode in $0.5M \text{ H}_2\text{SO}_4(\text{aq})$. Potentials are vs Hg/Hg₂SO₄ and 15-mV, 440-Hz modulation was used.

value of $\Gamma(\omega)$ over the spectral range of interest is about 0.030 eV for the model which we use here. The model spectra which are generated with no further parameter fitting for the variation of space-charge voltage are shown in Fig. 3. The qualitative fit to the experimental spectra is good as the line shape broadens with increasing depletion. The development of the shoulder on the low-energy peak is described, and the broadening on the low-energy peak is indicated. The evolution of the Franz-Keldysh oscillations is described as well as the structure due to the $E_0 + \Delta$ transition which is modeled by using a value of $B(E_0 + \Delta)$ one-third of that for the E_0 transition in accord with the work of Wysin *et al.*³¹ Although the reduction in peak height with increasing depletion is modeled well, the structure predicted on the main peak is not observed experimentally at -0.8 and -1.6 V versus Hg/Hg₂SO₄. The other main problem is that although the peak positions correlate well with theory at 1.2 V depletion, the experimental spectra narrow more rapidly on approach to flat band than is predicted. It was not possible to model this by using a different dopant density or by reducing the effective mass to the light-hole value of $0.034m_e$. We find this observation difficult to rationalize on either electrochemical or optical grounds.

The spectra for the nominally $4.4 \times 10^{17} \text{ cm}^{-3}$ *p*-type GaAs are shown in Fig. 4. Theoretical spectra were generated using the value of the dopant density derived from the Mott-Schottky plots of $2.7 \times 10^{17} \text{ cm}^{-3}$. The latter was used as the impedance behavior was classical in nature, and any deviations would be expected to lead to an overestimation of the dopant density due to surface-roughness effects and the contribution of surface-state charging to the differential capacitance. As can be seen from Fig. 5 and 6, the agreement between experiment and theory is good for the variation of shape, peak height, and peak position with applied potential if a flat-band potential of -0.25 V versus Hg/Hg₂SO₄ as measured from the impedance data is used. Γ_0 was decreased slightly to 0.009 eV in order to optimize the fit, but δ was not changed. The agreement between theory and experiment

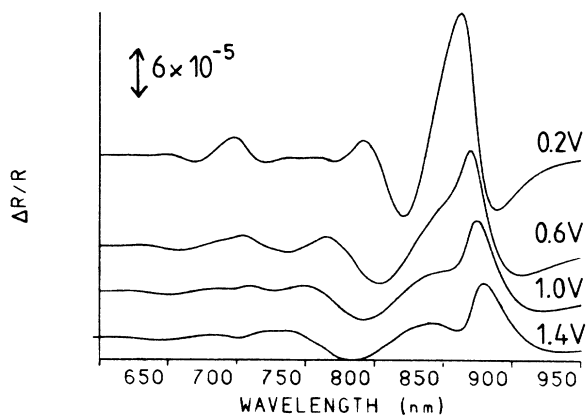


FIG. 5. Theoretical EER spectra for $2.7 \times 10^{17} \text{ cm}^{-3}$ p-type GaAs for various space-charge voltages. Calculated using $\Gamma_0 = 0.009 \text{ eV}$ and $\delta = 5 \text{ eV}^{-1}$.

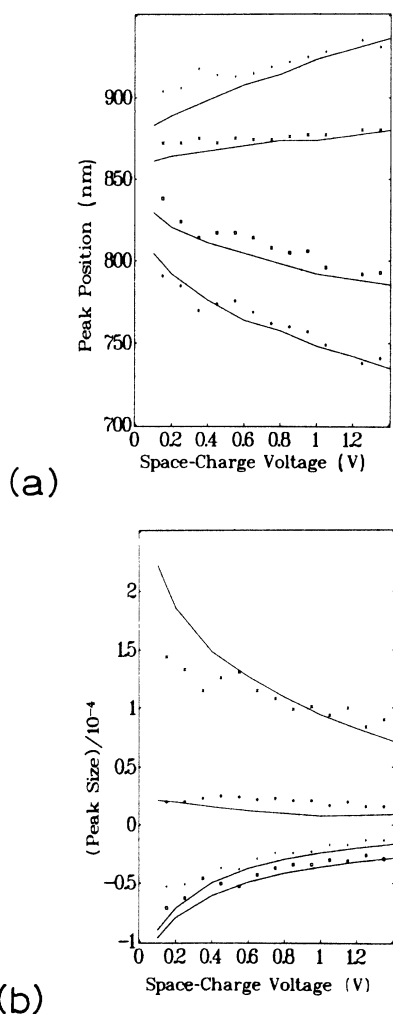
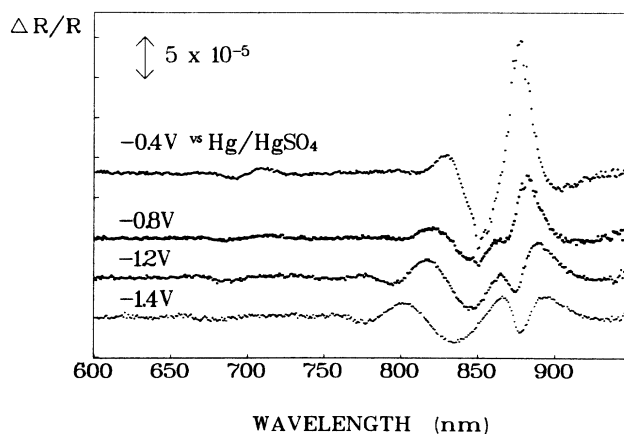


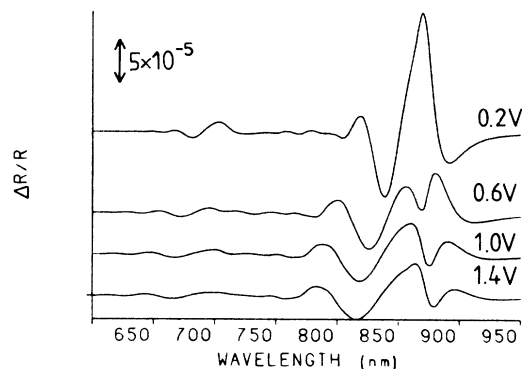
FIG. 6. (a) Plot of EER peak positions against space-charge voltage $V - V_{\text{FB}}$ for theoretical and experimental spectra of the $4.4/2.7 \times 10^{17} \text{ cm}^{-3}$ p-type GaAs. Theoretical values are represented by the solid lines and experimental values by the marked points. The impedance measured flat-band potential of $V_{\text{FB}} = -0.25 \text{ V}$ vs $\text{Hg}/\text{Hg}_2\text{SO}_4$ was used to calculate $V - V_{\text{FB}}$. (b) EER peak heights plotted against $V - V_{\text{FB}}$ for theory and experiment.

is a clear indication of the validity of our model and implies that any change in applied potential is dropped across the semiconductor space-charge layer.

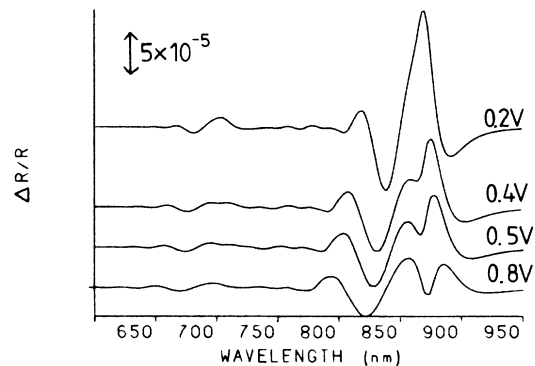
Theoretical spectra were generated for a dopant density of $7 \times 10^{16} \text{ cm}^{-3}$, Fig. 7(b), using the same values of Γ_0 and δ as above, but these bear little resemblance to the parallel experimental spectra if the Mott-Schottky-measured flat band of $+0.1 \text{ V}$ versus $\text{Hg}/\text{Hg}_2\text{SO}_4$ is used. The samples that were cut from this slice of p-type GaAs showed unstable impedance behav-



(a)



(b)



(c)

FIG. 7. (a) Experimental EER for 7×10^{16} p-type GaAs in $0.5 \text{ M H}_2\text{SO}_4$ 440 Hz and 15 mV. (b) and (c) Theoretical EER for $7 \times 10^{16} \text{ cm}^{-3}$ p-type GaAs for various space-charge voltages. $\Gamma_0 = 0.009 \text{ eV}$, $\delta = 5 \text{ eV}^{-1}$, and a modulation of 15 mV.

ior and considerable frequency dispersion of the Mott-Schottky plots. Only high-frequency measurements taken by rapidly sweeping the potential on fresh electrodes gave classical behavior which confirmed the manufacturer's dopant density and could sensibly be extrapolated back to estimate the flat-band potential. Electroreflectance spectra were also unstable and often appeared much reduced in size compared to others taken on the same sample and at the same potential. We consider this to be due to the presence of fast surface states which can fill and empty at the frequency of the applied modulation and cause only a portion of the voltage modulation to be dropped across the space-charge region. Although the spectrum size did vary for a given applied potential, depending on pretreatment, the line shape remained the same, implying that the space-charge voltage has a constant value for that applied potential. Several attempts were required to obtain the series depicted in Fig. 7(a), where each spectrum is the largest observed at that applied potential. The largest spectrum of any particular line shape should correspond to the situation where the greatest proportion of the voltage modulation is dropped across the space-charge region and should therefore be closest to the theoretical size.

Careful inspection reveals that predictions of the theory for $V_{SC}=0.2$ to 0.8 V, Fig. 7(c), closely parallel the experimental results for -0.3 to -1.3 V versus Hg/Hg₂SO₄. Comparison of the variation in peak position is shown in Fig. 8 using -0.1 V versus Hg/Hg₂SO₄ as the flat-band potential. The shift in flat-band potential from that measured by rapidly sweeping the applied potential away from flat-band under darkness was confirmed by impedance measurements under the conditions of EER. If the electrode is illuminated under typical EER light intensity and impedance is measured after allowing 10 min for equilibration at each potential, then results at high depletion give Mott-Schottky behavior which can be extrapolated back to a flat-band potential of approximately -0.2 V versus Hg/Hg₂SO₄. The shift does not result directly from the monochromatic EER illumination, which has no measurable affect if the potential is swept rapidly from flat band, but from allowing equilibration at each potential. In order to bring the theoretical peak positions into coincidence with similar experimental spectra we have incorporated a band-gap contraction of 0.007 eV into Fig. 8. Such a contraction could result from a high defect concentration near the surface³⁸ and was also used to interpret the EER of this sample in $1M$ KOH.

Comparison of the changes with V_{SC} predicted and those observed with applied potential very strongly suggests that only about 50% of any change in applied potential is actually dropped across the depletion layer. Thus, at -1.6 V versus Hg/Hg₂SO₄, which is about 1.4 V from the estimated steady-state flat-band potential, the electroreflectance spectrum implies $V_{SC}=0.8$ V. Similarly, at -0.6 V versus Hg/Hg₂SO₄, only 0.2 V appears to be dropped across the depletion layer.

Our results indicate that for 7×10^{16} cm⁻³ in $0.5M$ H₂SO₄ about 50% of any change in applied dc potential must be dropped across the Helmholtz layer

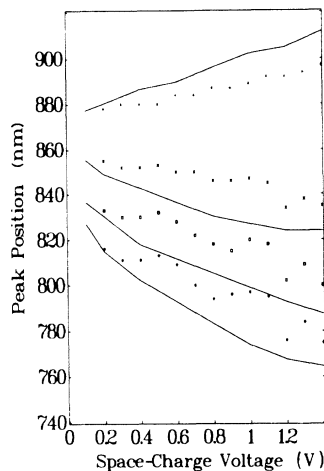


FIG. 8. Variation of EER peak positions for experiment and theory for 7×10^{16} cm⁻³ *p*-type GaAs with $V - V_{FB}$. A flat-band potential of $V_{FB} = -0.1$ V vs Hg/Hg₂SO₄ is chosen to give the best fit, and a band-gap contraction of 0.007 eV is included in the theoretical variation.

which can be described in terms of a high density of surface states that cause partial dc Fermi-level pinning. *These states must fill and empty relatively slowly in the case of the spectra shown in Fig. 7(a), as the size of the spectra corresponds closely to that predicted for each line shape.* The implication is that the 440-Hz potential modulation is too rapid to allow sufficient surface-state charging and discharging for a significant proportion of the potential modulation to be dropped across the Helmholtz layer.

Where spectra of similar shape, but reduced size were obtained, the density of *fast* surface states, which can respond to the modulation, has increased to a level where it reduces the potential modulation across the depletion layer. By using a higher modulation frequency, it should be possible to increase the proportion of the voltage modulation drop across the space-charge layer as the surface states become less able to fill and empty at the higher frequency. In principle, the kinetics of this process can be studied by variation of the modulation frequency and observation of the change in spectrum size. Unfortunately, the low-frequency range of our equipment and the high susceptibility of this behavior to change with time made such studies impractical for us in this case.

It is an important feature of the intermediate-field model that we have been able to deduce the presence of partial Fermi-level pinning from the line shape of the EER spectra, while the spectrum size has only corroborated the applicability of our model. It is also worth emphasizing that the ac impedance results were helpful only in demonstrating that a problem existed; we were unable to interpret data on equilibrated samples in terms of simple equivalent circuit models.

The structure and splitting of the low-energy peak has been observed commonly in GaAs ER where dopant densities are close to 10^{17} cm⁻³, but previously the lower-energy structure was assigned to impurity levels.³⁹⁻⁴³

However, our theoretical results show that such structures are in fact predicted by the classical electro-optic equations if the effect of the inhomogeneous electric field is included via a multilayer-reflection routine.

Impedance measurements confirmed the Hall-effect dopant density of the fourth sample as $2.0 \times 10^{18} \text{ cm}^{-3}$. However, theoretical spectra which were generated using this value were larger and broader than those obtained experimentally, Fig. 9. The broadness of the spectra in the intermediate-field regime is not significantly affected by the thermal broadening $\Gamma(\omega)$, unlike in the low-field limit. The shape of these theoretical spectra was not found to be sensitive to the size of voltage modulation below the 15 mV rms used, and $\Delta R/R$ scaled linearly with modulation amplitude, even when the space-charge voltage became small for theoretical spectra, so this cannot be the cause of any deviation from the calculated spectra. If the absorption is considered to be due entirely to excitation from the heavy-hole band, this would result in a slightly narrower theoretical line shape, but such an effect is nowhere near large enough to explain the deviation from experiment. The theoretical peak separations can therefore only be matched to those measured by either assuming that the space-charge voltage is very small,

as a result of Fermi-level pinning, or that the dopant density is less than the impedance analysis or Hall effect suggest. Either Fermi-level pinning or a lower dopant density would have the effect of reducing the electric field within the depletion layer.

The variation of peak position observed experimentally, see Fig. 9(a), with a change of applied potential of 0.7 V is consistent with space-charge voltages between 0.1 and 0.25 V for a dopant density of $2 \times 10^{18} \text{ cm}^{-3}$. For values of Γ_0 and δ as used for the other dopant densities, the theoretical $\Delta R/R$ values are far larger than those observed experimentally. The peak heights can be reduced by increasing thermal broadening to $\Gamma_0 = 0.050 \text{ eV}$ and $\delta = 1 \text{ eV}^{-1}$ and this will also cause the predicted peak heights to vary more slowly with space-charge voltage. A major disadvantage of altering Γ_0 and δ in this way is that the theoretical peaks which are predicted are rather formless in shape in contrast to those which were observed.

By using a dopant density of only $9 \times 10^{17} \text{ cm}^{-3}$ the variation of peak position with voltage can be modeled quite well without the assumption of any pinning processes. However, if the values of Γ_0 and δ used to interpret the other samples are used with the dopant density of $9 \times 10^{17} \text{ cm}^{-3}$, then again the peak heights predicted are far too large. The size of theoretical peaks can be reduced by increasing the thermal broadening $\Gamma(\omega)$, although this results in a loss of the structure of the peak shape. Once Γ_0 and δ have been set, the model then predicts the variation of the spectrum with applied voltage. The theoretical spectra shown in Fig. 9(b) were generated using $\Gamma_0 = 0.015 \text{ eV}$ and $\delta = 5 \text{ eV}^{-1}$, and the peak shape at higher depletion is well described, although on approach to flat band the increase in size of the main peak is greatly overestimated.

A further problem is the underestimation of the size of the minimum at $\sim 900 \text{ nm}$ compared to the main maximum at $\sim 860 \text{ nm}$, particularly close to the flat-band potential. We believe this latter point to be a general problem in applying our model to III-V compound semiconductors of dopant density $> 10^{18} \text{ cm}^{-3}$ as we have similar difficulty in interpreting the EER of such highly doped *n*-type GaAs, *n*-type $\text{Ga}_{1-x}\text{Al}_x\text{As}$, and *p*-type InP which have been communicated to us by Hutton and Peter.⁴⁴

It is difficult to be confident of any interpretation of our results for this highly doped material because of the differences between theory and experiment. Although significant errors can arise in the determination of the dopant density by Hall-effect and Mott-Schottky methods, the agreement of these two techniques does question the validity of the fitted value used in the EER theory in Fig. 9(b). The model used here does not appear to provide a quantitative account of the spectra for such highly doped samples. A possible reason for this is the doubt about the applicability of the equations for the bulk electro-optic effect to the multilayer model. As discussed earlier, deviations of theory from experiment due to this problem are most likely to be significant for samples of higher dopant density. It is clear that further theoretical work must be done in order to clarify this point.

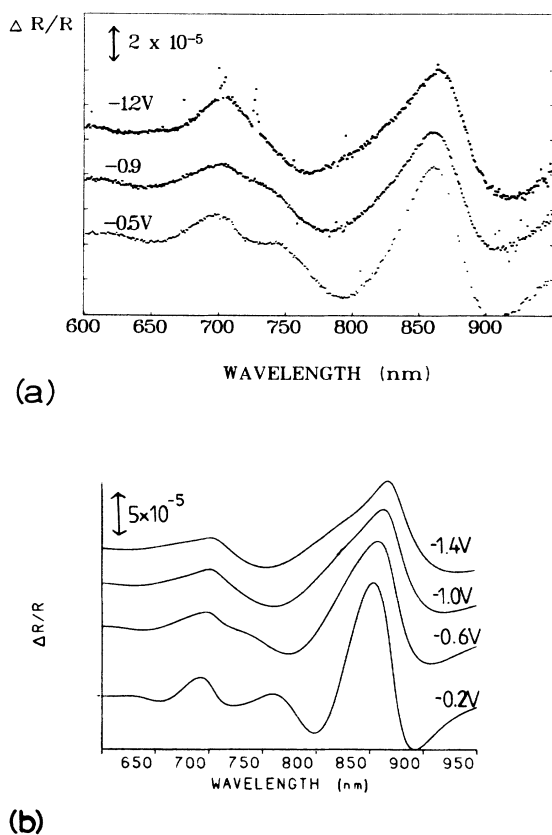


FIG. 9. (a) Experimental $2 \times 10^{18} \text{ cm}^{-3}$ *p*-type GaAs EER in $0.5M \text{ H}_2\text{SO}_4(\text{aq})$, 440 Hz 15 mV modulation and $\text{Hg}/\text{Hg}_2\text{SO}_4$ reference electrode. (b) Theoretical spectra for $9 \times 10^{17} \text{ cm}^{-3}$ *p*-type GaAs. $\Gamma_0 = 0.015 \text{ eV}$, $\delta = 5 \text{ eV}^{-1}$.

EER in 1M KOH (aq)

For all dopant densities the impedance behavior was very unstable in 1M KOH and it was difficult to obtain linear Mott-Schottky plots, even by sweeping the potential rapidly and using 10 000-Hz modulation. EER spectra had a tendency to be reduced in size compared to those taken in 0.5M H₂SO₄, especially if the electrode had been held at cathodic potentials. Particular difficulty was experienced in the potential region -1.1 to -1.5 V versus Hg/HgO where the electroreflectance spectra were often much reduced in size; this effect was most marked for the 2×10^{16} and 4.4×10^{17} cm⁻³ doped GaAs. However, spectra of similar size to those obtained in acid could generally be obtained reproducibly on either side of the potential range -1.1 to -1.5 V versus Hg/HgO, Fig. 10, if the electrode was held at open circuit before each scan. The results suggest that there is a high enough density of fast surface states close to the Fermi level at -1.2 V vs Hg/HgO to strongly diminish the 440-Hz potential modulation drop across the depletion layer.

If all the voltage modulation is dropped across the depletion layer, then the EER spectra should be of the same size as those observed in 0.5M H₂SO₄(aq), and correspond to those calculated theoretically. Even if a spectrum appears reduced in size, it is still possible to determine the depletion-layer voltage by comparison of line shape with theory and with results obtained in acid. Theoretical line shapes were not refitted for EER in 1M KOH(aq) as the line shapes were very similar to those obtained in acid, and any differences were seen to arise from differences in space-charge voltage. Indeed, it would be difficult to justify any changes in semiconductor parameters on moving between electrolytes, apart from possibly $\Gamma(\omega)$ which might be affected by the nature of the surface.

The line shape of 2×10^{16} cm⁻³ EER in 1M KOH(aq), Fig. 10, broadens more slowly with increasing cathodic applied dc potential than in 0.5M H₂SO₄(aq). This sug-

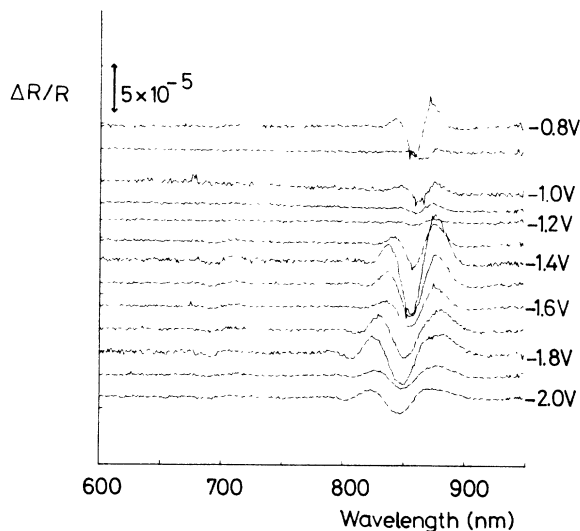


FIG. 10. Experimental EER for 2×10^{16} cm⁻³ p-type GaAs in 1.0M KOH(aq) with 440-Hz, 15-mV modulation and Hg/HgO reference electrode.

gests that only a proportion of any change in applied potential is dropped across the depletion layer in the former case. However, the rate at which the line shape broadens in 1M KOH(aq) is actually closer to that predicted, Fig. 3, than the more rapid separation of the peaks with potential seen in acid. The comparison of the changes of shape with applied potential between acid and base does suggest that only 75% of the change in V_{SC} in acid occurs in base for the same change in applied potential. However, in both cases we have no *firm* evidence that the majority of any change in applied potential is not dropped across the depletion layer.

We were unable to make any sensible estimate of the flat-band potential for 2.7×10^{17} cm⁻³ p-type GaAs from the impedance measurements which proved to be uninterpretable in terms of both two- and multi-component classical models. By assuming a flat-band potential of -0.8 V versus Hg/HgO spectra cathodic of -1.4 V versus Hg/HgO vary as predicted by the theory already shown in Fig. 5. Over the range -0.8 to -1.3 V the size of the EER spectra is much reduced compared to the model and acid data, and the line shape changes little with applied potential. Matching the theoretical line shapes to those observed suggests that the depletion-layer voltage is being rather strongly pinned between $V_{SC} = 0.4$ and 0.5 V. As a result, clear, large spectra can be obtained anodic of the nominal flat-band potential because the electrode is still in depletion. The flat-band potential moves to more anodic potentials as it is approached. This is illustrated by Fig. 11 which plots V_{SC} measured by comparison of spectra and peak positions for 1M KOH(aq) with theory and acid results, against the applied potential. The method is necessarily approximate although the variation of line shape with applied potential should allow us to estimate ϕ_{SC} to within 100 mV. Scatter in the points results from an uneven variation of the line shape with applied potential and slightly different line shapes at the same applied potential.

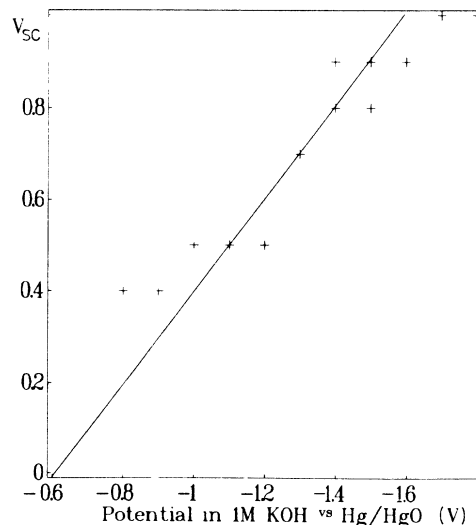


FIG. 11. Plot of EER measured space-charge voltage for 2.7×10^{17} cm⁻³ p-type GaAs in 1M KOH(aq) against the applied potential measured with respect to Hg/HgO.

EER spectra of $7 \times 10^{16} \text{ cm}^{-3}$ were prone to collapse in intensity in the range -1.2 to -1.5 V versus Hg/HgO. Several full sets of results were obtained and like those from $0.5 \text{ M H}_2\text{SO}_4(\text{aq})$ line-shape comparison with model spectra implied that only about half of any change in applied potential is dropped across the depletion layer. However, unlike the $0.5 \text{ M H}_2\text{SO}_4(\text{aq})$ case, spectra of different shape were obtained at the same applied potential for different scans, implying that V_{SC} can vary for a given applied potential. The irreproducibility of spectral line shape at a fixed applied potential suggests that the degree of Fermi-level pinning can vary and is very sensitive to the conditions in this system.

As in acid, these results are interpreted by assuming a band-gap contraction in order to bring theoretical peak positions into coincidence with the measured ones. Here we needed a contraction of 15 meV of the literature value of 1.425 eV .

The spectra for $2 \times 10^{18} \text{ cm}^{-3}$ samples in $1 \text{ M KOH}(\text{aq})$ proved to be very close to those seen in acid if an impedance-measured flat-band potential of -0.55 V versus Hg/HgO is used. The reduction in intensity in the region -1.2 to -1.5 V versus Hg/HgO was observed as for the other dopant densities in $1 \text{ M KOH}(\text{aq})$.

CONCLUSION

It is clear that the low-field approach of Aspnes does not apply to the EER of *p*-type GaAs which is presented here, as the line shape broadens and evolves with increasing depletion. However, if the intermediate-field theory of the effect is applied, and the inhomogeneous nature of electric field in the depletion layer is taken into account, then the spectra and their variation with potential can be successfully modeled. It is particularly important for the EER of the band-gap transition that the variation of the dielectric function within the depletion layer is included quantitatively, because the absorption coefficient is low enough for some of the incident light to penetrate through the depletion layer, and therefore the whole range of electric fields across the depletion layer is sampled.

The good correspondence between the model and the experimental EER spectra of some of the *p*-type GaAs samples in $0.5 \text{ M H}_2\text{SO}_4$ strongly suggests that most of any change in applied potential is dropped across the depletion layer of the semiconductor. Samples of dopant density $7 \times 10^{16} \text{ cm}^{-3}$ showed complex line-shape development which was closely predicted by our theory to occur over a potential range half the size of that actually observed. This is strong evidence that only about half of

any change in applied potential is dropped across the depletion layer and correlates with the unusually unstable impedance of these samples.

In the past, the type of structure which we observed has been attributed to the presence of impurity levels, but in fact the line shapes are predicted by the intermediate-field theory if parameters set in the spectra of lower-doped samples are used and the effect of the inhomogeneous field is included. Due to the rapid rate of change of line shape with space-charge voltage predicted by our theory, electroreflectance should be a particularly sensitive method of determining the space-charge voltage for both *n*- and *p*-type GaAs of dopant density $\sim 10^{17} \text{ cm}^{-3}$. Thus, it is possible to diagnose the presence of Fermi-level pinning in both electrolyte-semiconductor junctions and Schottky barriers from the *shape* of electroreflectance spectra. This model can similarly be applied to the interpretation of photoreflectance of bulk semiconductors.

The EER measured in 1 M KOH for *p*-type GaAs proved prone to collapse to much smaller size, particularly close to -1.2 V versus Hg/HgO. At other potentials the EER spectra often differed in size and shape from those found in acid electrolytes. Depending on pretreatment, even spectra obtained at the same formal potential on the same electrode showed considerable variability, though for no potential did the size of the spectra exceed that obtained in acid at the same formal depletion. Given the success of our approach in acid solutions, we were then able in alkali to distinguish between long-term Fermi-level pinning which affects the dc potential drop across the depletion layer, and faster pinning processes, which affect the size of the modulation across the depletion layer and therefore the size but not the shape of the EER spectrum.

By using a more complete physical model of the electroreflectance effect than has hitherto been applied, we have been able to interpret the spectra of *p*-type GaAs in electrolyte for a range of dopant densities. Our results enable us to effectively measure the depletion-layer voltage by the comparison of theoretical and experimental line shapes, and can therefore be used to directly identify band-edge unpinning.

ACKNOWLEDGMENTS

We should like to thank Dr. P. R. Trelvelick for instrumental help over the course of these experiments and Dr. S. J. Higgins for making the ellipsometric measurements referred to in the text.

¹W. H. Brattain and C. G. B. Garrett, *Bell Syst. Tech. J.* **34**, 129 (1955).

²N. F. Mott, *Proc. R. Soc. London, Ser. A* **171**, 27 (1939).

³W. Schottky, *Z. Phys.* **118**, 539 (1942).

⁴V. A. Myamlin and Yu. V. Pleskov, *Semiconductor Electrochemistry* (Plenum, New York, 1967).

⁵A. Fujishima and K. Honda, *Nature (London)* **238**, 37 (1972).

⁶A. Hamnett, in *Comprehensive Chemical Kinetics*, edited by G. Compton (Elsevier, Amsterdam, 1987), Vol. 27.

⁷M. Cardonna, *Modulation Spectroscopy* (Academic, New York, 1969).

⁸K. W. Frese, in *Semiconductor Electrodes, Studies in Physical and Theoretical Chemistry 55*, edited by H. O. Finklea (Elsevier, New York, 1988).

- ⁹D. E. Aspnes, Phys. Rev. **153**, 972 (1967).
- ¹⁰D. E. Aspnes, P. Handler, and D. F. Blossey, Phys. Rev. **166**, 921 (1968).
- ¹¹A. Hamnett, in Ref. 6, Vol. 29.
- ¹²D. A. B. Miller, D. S. Chemla, T. C. Damen, A. C. Gossard, W. Wiegmann, T. H. Wood, and C. A. Burras, Phys. Rev. B **32**, 1043 (1985).
- ¹³R. C. Bowman, R. L. Alt, and K. W. Brown, in *Proceedings of the Society of PhotoOptical Instrumentation Engineers*, Bay Point, 1987, edited by O. J. Glembocki, F. H. Pollak, and J. J. Song (SPIE, Bellingham, WA, 1987), Vol. 794, p. 194; R. Glosser and N. Bottka, *ibid.* p. 88.
- ¹⁴*Handbook of Mathematical Functions*, edited by M. Abramowitz and I. A. Stegun (Dover, New York, 1970).
- ¹⁵D. E. Aspnes, Surf. Sci. **37**, 418 (1973).
- ¹⁶B. R. Bennett and R. A. Soref, IEEE J. Quantum Electron. **QE-23**, 2159 (1987).
- ¹⁷D. E. Aspnes and A. Fropa, Solid State Commun. **7**, 155 (1969).
- ¹⁸R. N. Bhattacharya, H. Shen, P. Parayanthal, F. H. Pollak, T. Coutts, and H. Aharoni, Phys. Rev. **37**, 4044 (1988).
- ¹⁹W. K. Paik, in *MTP Review of Science*, Series One, edited by J. O'M Bockris (Butterworths, London, 1973), Vol. 6.
- ²⁰R. Del Sole and D. E. Aspnes, Nuovo Cimento B **39**, 802 (1977).
- ²¹R. Del Sole and D. E. Aspnes, Phys. Rev. B **17**, 3310 (1978).
- ²²R. P. Silberstein and F. H. Pollak, Solid State Commun. **33**, 1131 (1980).
- ²³R. P. Silberstein and F. H. Pollak, J. Vac. Sci. Technol. **17**, 1052 (1980).
- ²⁴D. E. Aspnes, Phys. Rev. B **10**, 4228 (1974).
- ²⁵P. M. Raccach, J. W. Garland, Z. Zhang, U. Lee, Da Zhong Xue, L. L. Abels, S. Ugur, and W. Wilinsky, Phys. Rev. Lett. **53**, 1958 (1984).
- ²⁶L. M. Abrantes, R. Peat, L. M. Peter, and A. Hamnett Ber. Bunsenges. Phys. Chem. **91**, 369 (1987).
- ²⁷*Landolt-Börnstein*, New Series, edited by O. Madelung (Springer-Verlag, Berlin, 1982), Vol. 17a, p. 218.
- ²⁸B. O. Seraphin and N. Bottka, Phys. Rev. **139**, 560 (1965).
- ²⁹M. Chandreskhar and F. H. Pollak, Phys. Rev. B **15**, 2127 (1977).
- ³⁰J. Bardeen, in *Photoconductivity Conference*, edited by R. G. Breckenridge, B. R. Russell, and E. E. Hahn (Wiley, New York, 1956).
- ³¹G. M. Wysin, D. L. Smith, and A. Redondo, Phys. Rev. B **38**, 12 514 (1988).
- ³²A. N. Pikhin and A. D. Yas'kov, Fiz. Tekh. Poluprovodn. **12**, 1047 (1978) [Sov. Phys.—Semicond. **12**, 622 (1978)].
- ³³D. D. Sell, H. C. Casey, and K. W. Wecht, J. Appl. Phys. **45**, 2650 (1974).
- ³⁴H. C. Casey, D. D. Sell, and K. W. Wecht, J. Appl. Phys. **46**, 250 (1975).
- ³⁵D. E. Aspnes and A. A. Studna, Phys. Rev. B **27**, 985 (1983).
- ³⁶B. E. Conway, H. Angerstein-Kozłowska, and W. B. A. Sharp, Anal. Chem. **45**, 1331 (1973).
- ³⁷D. E. Aspnes and A. A. Studna, Phys. Rev. B **7**, 4605 (1973).
- ³⁸S. M. Sze, *Physics of Semiconductor Devices*, 2nd ed. (Wiley, New York, 1981), p. 143.
- ³⁹B. O. Seraphin, Proc. Phys. Soc. London **87**, 239 (1966).
- ⁴⁰M. Cardona, F. H. Pollak, and K. L. Shaklee, Proceedings of the International Conference on the Physics of Semiconductors, Kyoto, 1966 [J. Phys. Soc. Jpn. Suppl. **21**, 89 (1966)].
- ⁴¹M. Cardona, K. L. Shaklee, and F. H. Pollak, Phys. Rev. **154**, 696 (1967).
- ⁴²E. W. Williams and V. Rehn, Phys. Rev. **172**, 798 (1968).
- ⁴³E. W. Williams, Solid State Commun. **7**, 541 (1969).
- ⁴⁴R. Hutton, Ph.D. thesis, University of Southampton, 1989.